

# Diffusion of water molecules in crystalline $\beta$ -cyclodextrin hydrates

K. Braesicke, T. Steiner, W. Saenger, and E.W. Knapp

Department of Biology, Chemistry, and Pharmacy, Institute of Chemistry, Freie Universität Berlin, Berlin, Germany

To understand the rapid diffusion mechanism of water molecules in the crystal lattice of hydrated  $\beta$ -cyclodextrin ( $\beta$ -CD), molecular dynamics (MD) simulations of crystalline  $\beta$ -CD were performed at five different relative humidities corresponding to hydration states ranging from  $\beta$ -CD- $9.4H_2O$  to  $\beta$ -CD- $12.3H_2O$ , and in aqueous solution. The trajectories for the crystalline  $\beta$ -CD hydrates had lengths of 4 ns each, whereas the simulation in aqueous solution extended to 2 ns. Transport of water molecules in the crystal was characterized in terms of a spatially varying diffusion constant and the main direction of diffusion, which were evaluated using newly developed algorithms. The main diffusion pathway winds through the cavities of adjacent doughnut shaped  $\beta$ -CD molecules and is slightly slanted with respect to the crystallographic *b*-axis. Water molecules outside the  $\beta$ -CD cavities have access to the main diffusion pathway. The diffusion constant for transport of water molecules along the main pathway calculated from the MD simulation data adopts 1/30 of the value in bulk water at room temperature. This is in agreement with estimates that can be made from experimental data on the adjustment of a  $\beta$ -CD crystal to changes in relative humidity. © 2000 by Elsevier Science Inc.

**Keywords:**  $\beta$ -cyclodextrin crystals, diffusion of water in crystals, diffusion pathway

## INTRODUCTION

The cyclodextrins (CD) are a family of macrocyclic oligosaccharides that are of interest in chemical research and pharmaceutical industries, because they are able to form inclusion complexes with molecules small enough to fit into their central cavities.<sup>1–4</sup> The commonly used  $\beta$ -CD consists of seven units of  $\alpha$ ,D-glucose connected by  $\alpha$ (1-4)-bonds. It has the shape of

Color Plates for this article are on pages 167–168.

Corresponding author: E.W. Knapp, Department of Biology, Chemistry, and Pharmacy, Institute of Chemistry, Freie Universität Berlin, Takustraße 6, 14195 Berlin, Germany. Tel.: 49-30-838-54387; fax: 49-30-838-53487.

E-mail address: knapp@chemie.fu-berlin.de (E.W. Knapp)

a flat truncated cone covered on both sides by hydroxyl groups. In crystal structures, different inclusion complexes of  $\beta$ -CD adopt different packing modes, which are determined by the nature of the guest molecules.<sup>5</sup> With small guest molecules such as simple alcohols or water, the  $\beta$ -CD molecules adopt a dense crystal packing in which both openings of the molecular cavity are closed by the surface of adjacent  $\beta$ -CD molecules. In this packing mode, the  $\beta$ -CD cavity forms an isolated molecular cage that is not directly connected with the cavities of neighboring molecules. In crystalline hydrated  $\beta$ -CD, this cage is filled with up to seven water molecules, which are disordered over 11 discrete positions. In addition, there are up to five water molecules per  $\beta$ -CD located in interstices between the  $\beta$ -CD molecules that can occupy eight different positions.<sup>5,6</sup> It was found with incoherent neutron scattering at room temperature that the disorder of the water molecules is dynamic in character, involving jump rates of about  $10^{10}$ – $11^{11}$  s<sup>-1</sup>.<sup>7</sup>

Crystal structures of  $\beta$ -CD hydrate were determined by X-ray structure analysis<sup>8</sup> at five different values of relative humidity. Accordingly, the water content varies from 9.4 water molecules per  $\beta$ -CD at 15% relative humidity to 12.3 water molecules at 100% relative humidity. The water content in the crystals adjusts within minutes to changes in relative humidity. On the basis of H/D and  $H_2O/D_2O$  exchange experiments, the diffusion constant was found to be about 1/60 of the corresponding value in bulk water.<sup>9</sup> This requires an efficient transport mechanism for the water molecules. Due to the dense packing of the  $\beta$ -CD molecules in the crystal, however, no static channel is visible where the water molecules could move freely. Hence, the rapid diffusion of the water molecules through the crystal lattice must be associated with a considerable degree of conformational flexibility of  $\beta$ -CD molecules, which may temporarily open suitable diffusion pathways.

Because crystalline  $\beta$ -CD hydrates may serve as interesting model systems to investigate how conformational flexibility and dynamic disorder can influence transport processes of cocrystallized water, we studied the motion of water molecules in the crystal lattice of  $\beta$ -CD hydrates by computer simulation of molecular dynamics (MD). The crystal was modeled by 24  $\beta$ -CD molecules with periodic boundary conditions. The MD trajectories of the crystal samples covered a total time span of 4 ns each and were generated at five different relative humid-

ties. For comparison of conformational flexibility in the aqueous phase, we also generated a trajectory of a single  $\beta$ -CD in a water box with periodic boundary conditions for a time period of 2 ns. MD simulations of  $\beta$ -CD crystals were performed previously,<sup>10</sup> but for technical reasons the simulation times of 20 ps were too short and the system size of eight  $\beta$ -CD molecules was too small to study the transport of water molecules through the crystal lattice.

The crystalline molecular system and the simulation techniques are described in greater detail in the Methods section. We demonstrate how a spatially varying diffusion constant and the main diffusion direction were evaluated for an inhomogeneous molecular system using specific and newly developed algorithms. In the Results and Discussion section, we provide an overview of the simulation data and of the diffusion of water molecules in the  $\beta$ -CD crystal lattice.

## METHODS

### Molecular System and Simulation Techniques

From aqueous solution,  $\beta$ -CD crystallizes in space group P2<sub>1</sub> with one  $\beta$ -CD molecule and 12 cocrystallized water molecules in each of the two asymmetrical units of the unit cell.<sup>5,6</sup> This is shown in Color Plate 1, which displays the crystal structure at 100% relative humidity. If exposed to an atmosphere of reduced relative humidity, the water content falls; the unit cell constants change accordingly, but the space-group symmetry P2<sub>1</sub> is maintained<sup>8</sup> (Table 1). The average number of water molecules per  $\beta$ -CD molecule is given in column seven of Table 1. For the crystalline molecular system, the computer simulation was performed for 12 unit cells containing 24  $\beta$ -CD and between 224 and 294 water molecules (Table 1). The model system was composed of two unit cells along the larger unit cell axes (a and c) and three unit cells along the shorter unit cell axis (b). Thus, the spatial extensions of the molecular system used for the MD simulation were a = 42 Å, b = 31 Å and c = 30 Å. Periodic boundary conditions were applied so that the molecular system satisfied translational symmetry. Six trajectories were generated to simulate MD of  $\beta$ -CD hydrate at different water contents. Five of these referred to crystals<sup>8</sup> at relative humidities of 15%, 42%, 58%, 78%, and 100%, and one to aqueous solution conditions. Coordinates of the nonhydrogen atoms of the  $\beta$ -CD molecules and of the oxygen atoms of the crystal water molecules were taken from the crystal structures of Steiner and Koellner.<sup>8</sup> The coordinates of the

hydrogen atoms were generated in ideal geometry by the H-build algorithm of CHARMM.<sup>11</sup> Torsion angles involving hydrogen atoms were varied on a grid to minimize the energy.

To simulate the dynamics of  $\beta$ -CD in aqueous solution, a single  $\beta$ -CD molecule was put into a 40 Å × 40 Å × 40 Å cube of water molecules. The coordinates of the  $\beta$ -CD molecule were taken from the crystal structure at 100% relative humidity. Water molecules with oxygen atoms closer than 2.5 Å to any nonhydrogen atom of the  $\beta$ -CD molecule or to one of the water oxygen atoms from the crystal structure were removed. The total number of water molecules remaining in the system was 2026. Periodic boundary conditions were applied.

For all computer simulations, the CHARMM22 energy function<sup>12</sup> was used. The water molecules were parameterized with the SPC/E water model.<sup>13</sup> Atomic partial charges of the  $\beta$ -CD molecules, which generate the electrostatic potential outside of the molecule appropriately, were calculated with SPARTAN<sup>14</sup> using the 6-31G\* basis set by optimizing the geometry of a fragment formed by three a(1→4)-linked D-glucoses. The calculated charges of the central D-glucose unit from the trimeric  $\beta$ -CD fragment are given in the legend of Figure 1.

To save CPU time, all nonbonded interactions were smoothly turned off by the atom group switch function with a start distance of 11.5 Å and a cut-off radius of 13.0 Å.<sup>12</sup> This cut-off radius value is optimized to obtain a correct value of the diffusion constant in bulk water, if the SPC/E water model is used.<sup>15</sup> The reservoir radius of the nonbonded neighbor list extended to 17 Å, and this list was updated every fifth time step.

Before the atomic coordinates of the molecular systems were used to simulate the dynamics, possible strain had to be released by energy minimization. This was done in two steps. In the first step, the coordinates of all hydrogen atoms were improved by energy minimizing the molecular system while the coordinates of all nonhydrogen atoms were fixed to their values given by the crystal structure. In the second minimization step, all constraints were released.

In the initial 60 ps time interval of the computer simulation, the molecular system was heated to a temperature of 300K. For this purpose, the velocities of each atom were rescaled in time steps of 0.2 ps to increase the temperature of the molecular system derived from the total kinetic energy by 1K. Subsequently, the system was allowed to reach thermal equilibrium within 140 ps. In this time period, the velocity of each atom was rescaled only if the temperature average in a 2 ps time

**Table 1. General data on crystals of  $\beta$ -cyclodextrin hydrates<sup>8</sup>**

Humidity h [%]	a Axis [Å]	b Axis [Å]	c Axis [Å]	$\beta$ angle $\angle(a,c)$ [°]	Total volume V(h) [Å <sup>3</sup> ]	No. H <sub>2</sub> O per $\beta$ -CD n(h)	$\Delta V(h)^*$ [Å <sup>3</sup> ]	No. H <sub>2</sub> O per 24 $\beta$ -CD
100	21.283	10.322	15.092	112.41	3065	12.26	0	294
78	21.233	10.294	15.103	112.22	3056	11.89	-13	285
58	21.161	10.254	15.110	111.91	3042	11.56	-19	275
42	21.080	10.192	15.131	111.58	3024	11.19	-23	269
15	20.857	10.158	15.140	110.94	2996	9.35	-106	224

\* $\Delta V$  is the difference between the observed change of the unit cell volume,  $V(100\%) - V(h)$ , and the volume change expected from the change in the water content  $\Delta n(h) = n(100\%) - n(h)$  if the volume of a water molecule is considered to be  $V_{H_2O} = 30.028\text{Å}^3$ . Because there are two  $\beta$ -CD molecules per unit cell, we obtain  $\Delta V(h) = V(100\%) - V(h) - 2 \Delta n(h) \cdot V_{H_2O}$ . The negative volume changes in column eight indicate that the crystals at high relative humidity are more densely packed.

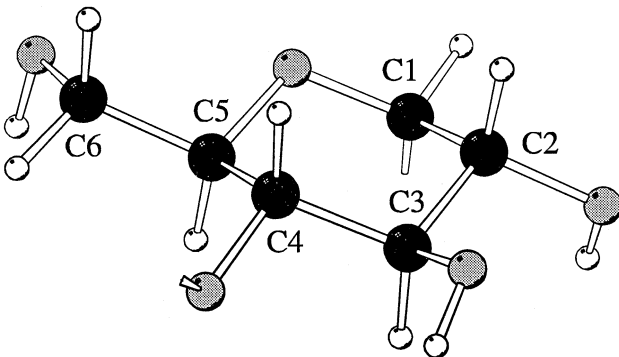


**Figure 1.** Glucose unit of the  $\beta$ -CD molecule. Carbon atoms are shown in black, oxygen atoms in gray, and hydrogen atoms in white. The corresponding atomic partial charges calculated on the 6-31G\* level<sup>14</sup> are: C1 0.399, H1 0.082, C2 0.085, H2 0.085, O2 -0.628, HO2 0.420, C3 0.358, H3 0.052, O3 -0.671, HO3 0.420, C4 0.096, H4 0.016, O4 -0.557, C5 0.352, H5 0.040, O5 -0.578, C6 0.271, H61 0.020, H62 0.020, O6 -0.686, HO6 0.404.

interval was outside of the temperature window of  $(300 \pm 10)$ K. After the initial time period of 200 ps, rescaling of the velocity of the atoms to adjust the temperature of the molecular systems was no longer performed. The integration step used for the time propagation was 2 fs throughout. This large integration step was possible because the bond lengths involving hydrogen atoms were constrained by the SHAKE algorithm.<sup>16</sup> The values of temperature, energy, and atomic coordinates were stored every 0.2 ps.

## Diffusion Process

The transport behavior of water molecules in crystalline  $\beta$ -CD hydrates was characterized by evaluating the spatially dependent diffusion constant and the main diffusion direction of the MD simulation data. For this purpose, the diffusion constant was calculated on the grid points of a regular lattice. For molecular systems with inhomogeneous diffusion conditions, the Einstein relation, valid for homogeneous diffusion,  $6DT = \langle [\vec{r}(0) - \vec{r}(t)]^2 \rangle$ , is not suitable to evaluate diffusion constants. Thus, another procedure had to be developed. Nevertheless, the starting point of the description was still the diffusion equation for a homogeneous molecular system without sources and with vanishing stationary current as defined by Equation 1:

$$\frac{\partial C}{\partial t} = D\nabla^2 C, \quad (1)$$

where  $D$  is the diffusion constant and  $C(\vec{r}, t)$  is the probability distribution of the water molecules at position  $\vec{r}$  and time  $t$ . For a spatially inhomogeneous system, the diffusion constant is calculated by monitoring how tagged water molecules move through the surface of a small probe sphere with radius  $a$  into the total molecular system represented by the system sphere with a large radius  $b >> a$ . The system sphere is closed by imposing reflecting boundary conditions:

$$\left. \frac{\partial C}{\partial r} \right|_{r=b} = 0. \quad (2)$$

Initially we assume a probability distribution of tagged water molecules:

$$C(\vec{r}, t=0) = \begin{cases} \frac{3}{a^3} & 0 \leq r \leq a \\ 0 & a < r < b \end{cases} \quad (3)$$

within the probe sphere. These water molecules leave the probe sphere with time. The total concentration of water molecules left in the probe sphere after time  $t$  is:

$$n(t) = \int_{\text{probe sphere}} C(\vec{r}, t) d^3r, \quad (4)$$

yielding the analytically exact expression<sup>17</sup>:

$$n(t) = \frac{a^3}{b^3} + \sum_{k=1}^{\infty} s_k^2 \exp\left(-\frac{\mu_k^2}{b^2} Dt\right). \quad (5)$$

The radius of the system sphere is given by the ratio of volumes of the probe sphere  $V_a$  and of the total molecular system  $V_b$ :

$$b = a \left( \frac{V_b}{V_a} \right)^{1/3}. \quad (6)$$

The linear expansion coefficients  $s_k^2$  are given as:

$$s_k^2 = 6 \frac{b^3 (1 + \mu_k^2)}{\mu_k^6} \left( \sin \frac{\mu_k a}{b} - \frac{\mu_k a}{b} \cos \frac{\mu_k a}{b} \right)^2, \quad (7)$$

where the  $\mu_k$  are solutions of the transcendental equation  $\tan \mu = \mu$ . In the present application, the radius  $b$  of the total molecular system was larger by two orders of magnitude than the radius  $a$  of the probe sphere. Under these conditions, the time decay of  $n(t)$ , Equation 5, does not depend on the exact size of the system sphere, and it does not matter whether the actual molecular system has periodic or spherical boundary conditions. The dependence of the time decay pattern of  $n(t)$  on the radius  $b$  of the system sphere is shown in Figure 2. In all our applications, it was of sufficient accuracy to evaluate the infinite sum (Equation 5) for at most 300 terms.

The diffusion constant was determined by minimizing  $[n_{MD}(t) - n_{theory}(t)]^2$ , where  $n_{MD}(t)$  is the time-dependent concentration of water molecules derived from computer simulation and  $n_{theory}(t)$  is the corresponding value from the analytical expression (Equation 5). The concentrations used to determine the diffusion constant were derived as an average over the last 3 ns of an MD trajectory of 4 ns time length considering 1500 time origins taken every 2 ps. If at a given point a water molecule was found in the probe sphere for only five time origins and less, or if  $n_{MD}(T = 10 \text{ ps}) < 10^{-6}$ , the calculated diffusion constants are subject to large statistical errors and negligible. Consequently, no diffusion constant and pathway were determined at this point.

The radius  $a$  of the probe sphere should be small enough to yield sufficient spatial resolution and large enough to guarantee statistically significant results. To find an appropriate value, the radius was varied from  $a = 0.6$  to  $1.0 \text{ \AA}$ . Figure 3 shows an example of the time dependence of the relative concentrations of  $n_{theory}(t)$  and  $n_{MD}(t)$  with different values of the radius  $a$  of the probe sphere for MD simulation data at 15% relative humidity. This example refers to a reference point  $(x_1, y_1, z_1)$  on the main diffusion pathway in one of the  $\beta$ -CD macro-

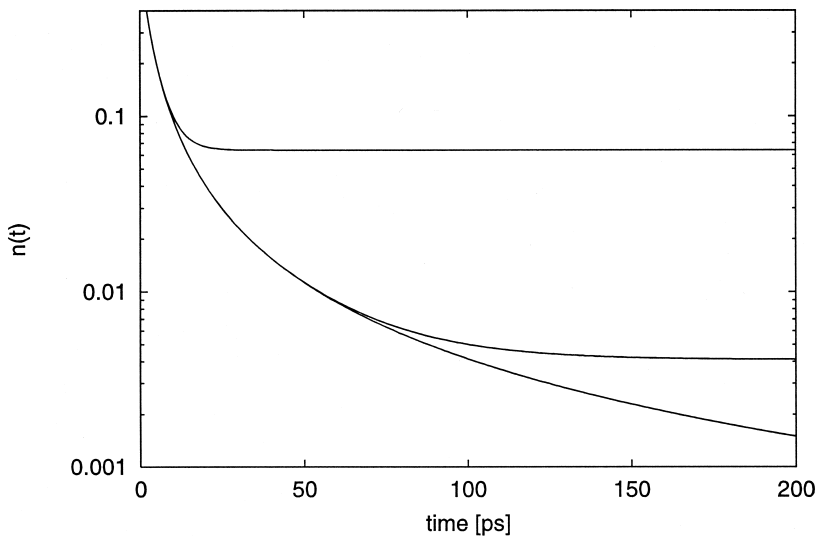


**Figure 2.** Dependence of the time decay pattern of  $n_{\text{theory}}(t)$ , Equation 5, for different radii  $b$  of the large system sphere. The radius  $a$  of the probe sphere is  $0.8 \text{ \AA}$  and the value of the diffusion constant is  $D = 0.05 \text{ \AA}^2/\text{ps}$ . For smaller values of the diffusion constant, the differences would appear at even larger times. From top to bottom, the radii of the system sphere are  $2.0$ ,  $5.0$ ,  $10.0$ , and  $100.0 \text{ \AA}$ . For the two largest values of radius  $b$  ( $10.$  and  $100.$   $\text{\AA}$ ), the corresponding curves cannot be discriminated.

cycles. The value of the diffusion constant determined by this procedure was essentially independent of the radius of the probe sphere within the interval  $0.6$ – $1.0 \text{ \AA}$ . Table 2 shows how

the calculated values of the diffusion constant and the main directions of the diffusion depend on the size of the probe sphere. Because the dependence found for the direction and

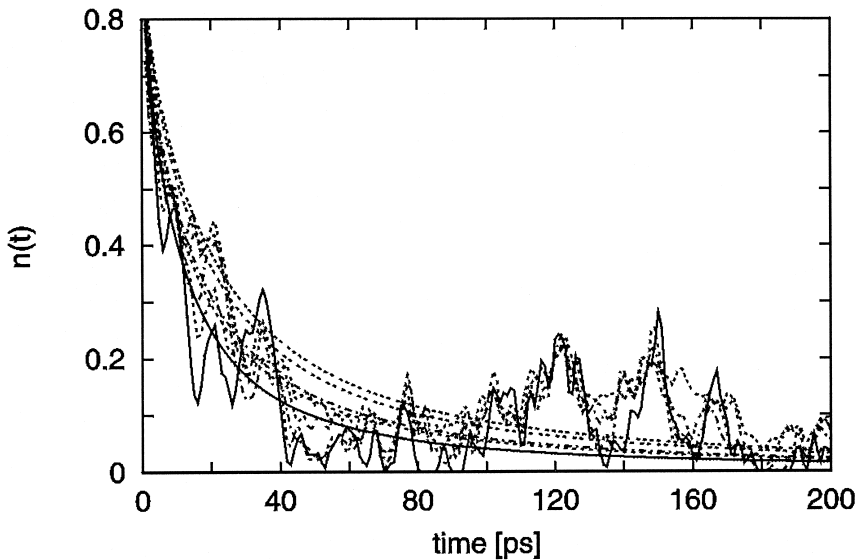


**Figure 3.** Variation of time dependence of the relative concentration  $n(t)/n(0)$  of water molecules with different sizes of probe sphere. The radius  $a$  of the probe sphere was varied from  $0.6$  to  $1.0 \text{ \AA}$  in steps of  $0.1 \text{ \AA}$ . The corresponding five samples of  $n_{\text{MD}}(t)$  refer to one MD simulation data set at  $15\%$  relative humidity for a reference point  $(x_1, y_1, z_1)$  on the main diffusion pathway in the center of one  $\beta$ -CD macrocycle. The analytically evaluated concentration dependencies  $n_{\text{theory}}(t)$  (smooth and monotonously decaying curves) were evaluated from the analytical expression (Equation 5) and compared with corresponding simulation data  $n_{\text{MD}}(t)$  (nonmonotonously decaying curves) using the best fit of the diffusion constant. From top to bottom, the concentration dependencies  $n_{\text{theory}}(t)$  refer to increasing radii of the probe sphere. For equivalent data from MD simulation and theory, the same line style is used. The values of the diffusion constant varied between  $0.0055$  and  $0.0084 \text{ \AA}^2/\text{ps}$  (Table 2), demonstrating that the variation with the radius of the probe sphere is small and that a radius of  $a = 0.8 \text{ \AA}$  for the probe sphere is appropriate.

**Table 2.** Values of diffusion constant and main direction for different radii of probe sphere

Radius a [Å]	0.6	0.7	0.8	0.9	1.0
D [Å <sup>2</sup> /ps]	0.0055	0.0061	0.0074	0.0075	0.0084
Direction $\varphi$ [°]	237	240	237	240	237
Direction $\vartheta$ [°]	77	77	75	75	77

The diffusion is measured at the reference point ( $x_1, y_1, z_1$ ) located along the main diffusion pathway in one of the  $\beta$ -CD rings. Angle  $\varphi$  defines longitude and angle  $\vartheta$  latitude of the main direction of diffusion at the reference point. The probe sphere is orientated in the crystal such that its equator is positioned parallel to the plane defined by the crystal axes a and c.  $\varphi = 0^\circ$  is in direction of the crystal axis c and  $\vartheta = 0^\circ$  is approximately parallel to the crystal axis b.

magnitude of the diffusion process is small,  $a = 0.8 \text{ \AA}$  seems to be an appropriate value for the radius of the probe sphere.

The spacing of the grid points on which the diffusion constant was determined had to be small enough to allow the diffusion pathway to be followed in detail and large enough to limit time-consuming computations. Figure 4 shows the variation of the time decay of concentrations  $n_{\text{theory}}(t)$  and  $n_{\text{MD}}(t)$ , if the origin of the probe sphere is displaced along the three crystallographic axes by  $0.4 \text{ \AA}$  from the reference point ( $x_1, y_1, z_1$ ) considered before. The variations of the values of the diffusion constant and the directions of diffusion are small (Table 3). Consequently, a lattice of  $84 \times 62 \times 60$  grid points and  $0.5 \text{ \AA}$  grid spacing was used to calculate the diffusion constants to spatially resolve the whole molecular system, whose size is  $42 \text{ \AA} \times 31 \text{ \AA} \times 30 \text{ \AA}$ .

## Diffusion Pathway

To characterize the diffusion pathway, it is necessary to find the directions with the largest diffusion constant at each grid

**Table 3.** Values of diffusion constant and main direction for small displacements of probe sphere

Displacement from (0, 0, 0) ( $x_1, y_1, z_1$ ) [Å]	(0.4, 0, 0)	(0, 0.4, 0)	(0, 0, 0.4)
D [Å <sup>2</sup> /ps]	0.0074	0.0058	0.0055
Direction $\varphi$ [°]	237	225	235
Direction $\vartheta$ [°]	75	70	73

Small displacements from the reference point are considered. For further information, see legend to Table 2.

point. For this purpose, the surface of the probe sphere was partitioned in small and even tiles. Such a partition scheme requires:

- For each tile, there must be a tile in opposite direction.
- For each ray emanating at the center of the probe sphere, it must be easy to determine through which tile it will pass.

Regular polyhedra available for this purpose are listed in Table 4 with their types and number of surface elements. However, even the icosahedron has a very limited angular resolution of  $22.5^\circ$  only. Therefore, we are choosing an icosahedron, whose tiles are partitioned further in four smaller tiles as indicated by the thin lines in Figure 5. Hence, there are 80 tiles, which consequently cover a spatial angular range of  $4\pi/80$ , providing an angular resolution of better than  $12^\circ$ . The tiles are nearly equal in size, with a variation less than 5%. The numbering of the tiles runs from 0 to 79. It is organized similarly as for a dice in such a way that the sum of numbers on each pair of opposite tiles is 79. With this algorithm, the main direction of diffusion was calculated at each grid point considering a probe sphere with the radius  $a = 0.8 \text{ \AA}$ .

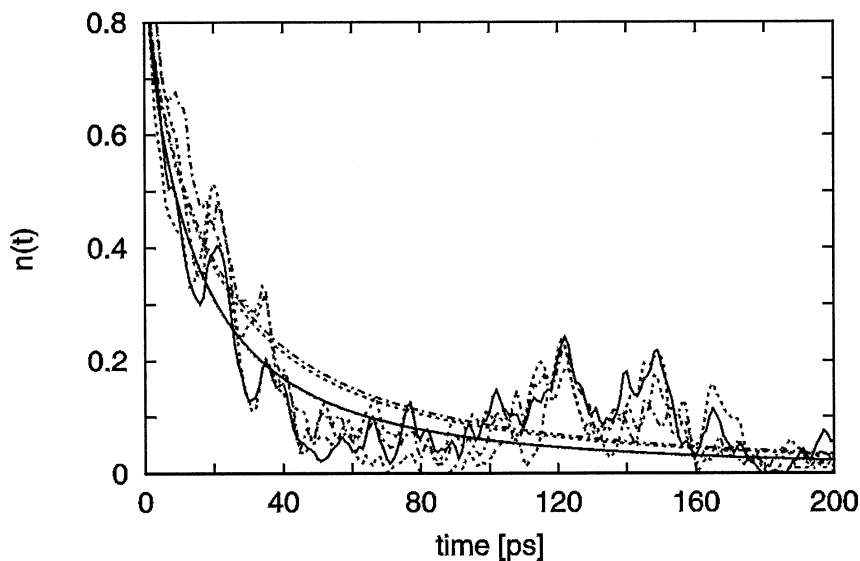


*Figure 4.* Spatial variation of the time decay of the relative concentration  $n(t)/n(0)$  of water molecules. The same MD simulation data as in Figure 4 were used. The spatial variation of  $n(t)$  is shown for a probe sphere of radius  $a = 0.8 \text{ \AA}$  placed at the same reference point ( $x_1, y_1, z_1$ ) considered in Figure 3 and by displacing the probe sphere from there by  $0.4 \text{ \AA}$  along the positive directions of the three crystal axes. The corresponding values of the diffusion constants are given in Table 3. From top to bottom, the concentration dependencies  $n_{\text{theory}}(t)$  refer to displacements (0,0.4,0), (0.4,0,0), (0,0,0), and (0,0,0.4). For more details, see legend to Figure 3.

**Table 4. Regular polyhedra**

Body	No. of surfaces	Type of surface
Tetrahedron	4	Equilateral triangle
Cube	6	Square
Octahedron	8	Equilateral triangle
Dodecahedron	12	Pentagon
Icosahedron	20	Equilateral triangle

Table 3 shows how the main directions of diffusion depend on small displacements from the reference point ( $x_1, y_1, z_1$ ). Once the main diffusion directions were calculated for each grid point, the diffusion pathways can be characterized by generating traces of the diffusion pathway consisting of straight line elements using the following algorithm, which is applied to a lattice with a grid spacing of 0.5 Å as used in the present application:

1. Start with a reference point at an arbitrary position in the molecular system.
2. Check the grid point nearest to the reference point. If no diffusion constant can be determined for this grid point because it is located within the atomic skeleton of one of the β-CD, stop the procedure. Else, move the reference point 0.25 Å in the main direction of diffusion determined for this grid point to reach a new position in space.

3. Repeat step 2 for the new reference point up to 40 times. This is sufficient to reach the end point of any individual diffusion pathway.

The resulting individual diffusion pathway was stored if its diameter was larger than 4.5 Å, where the diameter of a path is defined as the maximum distance between two positions on the path. The algorithm was applied by using each grid point of the lattice placed on the molecular system as a starting position.

In a second step, another algorithm was used that combines the diffusion pathways obtained with the preceding algorithm:

- Transform all diffusion pathways into the same unit cell by using the translational symmetry of the crystal. Duplicate all pathways in accordance with the crystal space group P2<sub>1</sub>.
- Connect all pathways whose ends are closer than 0.2 Å and whose final directions differ by less than 45°.
- Arrange the resulting diffusion pathways according to visual inspection.

## RESULTS AND DISCUSSION

### Overview and Quality Control

To demonstrate the quality of the simulation data, the time course of temperature and root mean square deviation (RMSD) of the simulated molecular systems are depicted. To obtain a better overview of the simulation data, the data sets of temper-

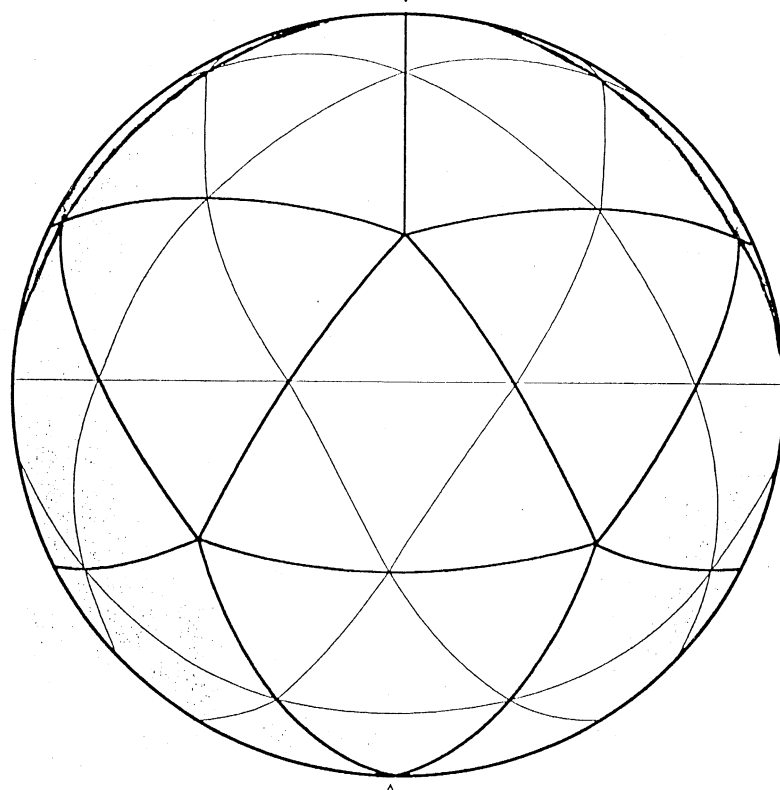
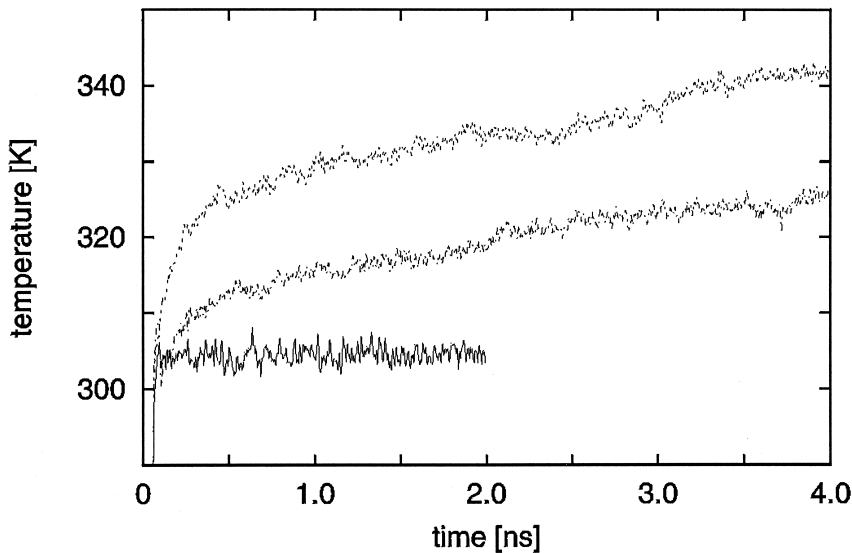


Figure 5. Partitioning of the surface of a probe sphere by 80 even tiles. The triangular surfaces of the icosahedron projected on the surface of the probe sphere are shown with thick lines. The thin lines demonstrate how these spherical triangles are partitioned in four smaller triangular tiles. See text for details.



**Figure 6.** Time dependence of the temperature of the MD simulation data. The curve extending up to 2 ns refers to the MD simulation of a single  $\beta$ -CD molecule in water. The other two curves represent simulation data of the crystalline molecular systems with 15% (lower curve) and 100% relative humidity (upper curve).

ature and RMSD are smoothed by averaging over time intervals of 8 ps involving 40 data points each.

The temperature is determined from the value of the kinetic energy as follows<sup>18</sup>:

$$k_B T = \frac{1}{3N_{\text{atom}} - N_{\text{constr}}} 2E_{\text{kin}}, \quad (8)$$

where, for instance,  $N_{\text{atom}} = 4410$  is the total number of atoms in the crystalline molecular system at 100% relative humidity and  $N_{\text{constr}} = 2562$  the number of constraining conditions, which in the present case is the number of fixed bond lengths involving hydrogen atoms.

Figure 6 displays the temperature as a function of time for the MD simulations of  $\beta$ -CD in water with a simulation length of 2 ns and of two crystalline systems consisting of 24  $\beta$ -CDs at 15% and 100% relative humidity with a simulation period of 4 ns. The temperature values in the simulations for the other crystalline systems at intermediate humidities of 42%, 58%, and 78% lie between the temperature curves for 100% and 15% relative humidity. In the initial time period of heating and equilibration, the temperature increases rapidly. Subsequently, the temperature increases only slowly with time for all molecular systems considered. In this time regime, ranging from 1 to 4 ns for the crystalline samples, the temperature remains in a relatively narrow range whose width is not larger than 11 K, as shown in Table 5. The temperature increase is typically due to release of strain in the molecular system, which increases the kinetic energy at the expense of potential energy. However, at the same time a small increase in the total energy can be observed, which is due to sudden conformational changes after release of strain whose motion cannot be resolved sufficiently by the time propagation algorithm. The average temperature of the molecular systems increases with increasing relative humidity of the crystalline sample, presumably because there is more strain that relaxes more slowly in the more densely

packed molecular systems at larger relative humidity. That the more humid crystalline samples are more densely packed is shown in column eight of Table 1.

Generally, a time period of about 1 ns was needed for heating and subsequent equilibration of MD simulation of the crystalline molecular systems, whereas only 300 ps was needed for these processes if a single  $\beta$ -CD molecule in the liquid phase was considered. The remaining time interval of the MD simulation data, which is 1 to 4 ns for the crystalline samples and 300 ps to 2 ns for a single  $\beta$ -CD molecule in aqueous solution, was used for evaluation of the diffusion constants and the diffusion pathways.

The RMSD values of a single  $\beta$ -CD molecule were calculated according to:

$$\text{RMSD}(t) = [\langle \text{MSD}(t) \rangle_{\text{atoms}}]^{1/2} = \left[ \frac{1}{N} \sum_{i=1}^N (\bar{r}_{\text{cryst},i} - \bar{r}_{\text{MD},i}(t))^2 \right]^{1/2} \quad (9)$$

**Table 5. Averaged value of diffusion constant on the diffusion pathway**

Humidity h [%]	Temperature interval T [K]	Average diffusion constant D [ $\text{\AA}^2/\text{ps}$ ]
100	330–342	$0.0062 \pm 0.0032$
78	324–332	$0.0083 \pm 0.0068$
58	332–340	$0.0057 \pm 0.0041$
42	324–334	$0.0065 \pm 0.0032$
15	314–325	$0.0059 \pm 0.0039$

The temperature interval yields the initial and final temperature values corresponding to the simulation data in the time interval from 1 to 4 ns used to evaluate the diffusion processes.

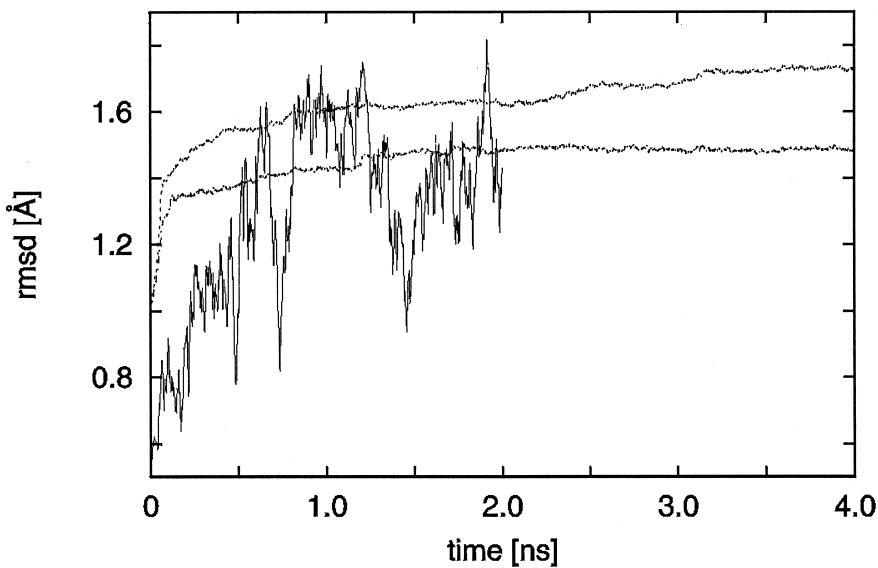


Figure 7. Time dependence of the rmsd with respect to the crystal structure of  $\beta$ -CD hydrate. MD simulation data of the same molecular systems considered in Figure 6 are depicted.

The coordinates of the  $i$ -th atom of the  $\beta$ -CD molecule in the crystal structure are given by  $\vec{r}_{\text{cryst},i}$ , whereas  $\vec{r}_{\text{MD},i}(t)$  are the coordinates of the corresponding atoms in the MD simulation data at time  $t$ . The Kabsch algorithm<sup>19</sup> was applied to remove translational and rotational displacements of the molecule by using the best fit of the instantaneous MD coordinates of the  $\beta$ -CD atoms with respect to its crystal structure coordinates. The sum in Equation 9 runs over all nonhydrogen atoms of the  $\beta$ -CD molecules considered in the molecular system.

Figure 7 depicts the RMSD of the  $\alpha$ ,D-glucose ring atoms of  $\beta$ -CD in water and in crystalline environment with 15% and with 100% relative humidity as a function of time. The RMSD values for the other crystalline samples at relative humidities of 42%, 58%, and 78% lie between the RMSD values for 100% (upper curve) and for 15% relative humidity (lower curve). The amplitudes of the fast oscillations in the time dependence of the RMSD, which are superimposed on the gradual increase of the average RSMD, are a measure of the fluctuations of the spatial positions of the atoms of the  $\beta$ -CD molecules. The average RMSD of a single  $\beta$ -CD in water possesses larger fluctuations for two reasons:

1. There is no averaging over 24  $\beta$ -CD molecules as for the crystalline samples.
2. The  $\beta$ -CD molecules are more mobile in an aqueous than in a crystalline environment.

The average molecular fluctuations of the  $\beta$ -CD atoms, i.e., those without free translations and rotations, obtained from the MD simulation in aqueous solution, agree with the average value derived from the B-factors of the crystal structures of hydrated  $\beta$ -CD. Although the B-factors also contain contributions from displacements and reorientations of  $\beta$ -CD molecules in the crystal, this agreement is an indication of a large degree of flexibility of the  $\beta$ -CD molecules within the crystal, which can facilitate the transport of water molecules through the crystal lattice.

The total RMSD values of  $\beta$ -CD molecules are smaller for a single  $\beta$ -CD in the aqueous phase than for 24  $\beta$ -CDs in the

crystalline phase, because in the crystalline phase there also are contributions from translational and orientational disorder of the 24  $\beta$ -CD molecules relative to each other. The RMSD values of the  $\beta$ -CD ring atoms are larger than the values obtained for the backbone atoms of proteins, which typically are in the range from 1.0–1.2 Å. The main reason for the larger RMSD values of the  $\beta$ -CD is probably that the CHARMM force field is not particularly adjusted to describe carbohydrate molecules. Another reason could be that the annular structure of the  $\beta$ -CD macrocycle is more flexible than the native conformation of a densely packed globular protein.

## Diffusion Constant and Diffusion Pathway

The dependence of the average diffusion constant along the main diffusion pathway as a function of the relative humidity is given in Table 5. Due to the relatively large uncertainty of these values, no clear trend of this dependence becomes visible, though there is a tendency for the mobility of water molecules to decrease with lower relative humidity. Such effects generally occur in biomolecular systems and particularly in proteins, which become less flexible and lose their functional behavior when kept under dry conditions.<sup>20</sup> The value of the calculated diffusion constant along the main diffusion pathway is about  $0.007 \text{ \AA}^2/\text{ps}$ <sup>21</sup> when averaged over the crystalline samples simulated at different water content. In an X-ray diffraction experiment on a  $\beta$ -CD crystal of dimensions  $0.4 \text{ mm} \times 0.3 \text{ mm} \times 0.2 \text{ mm}$ , at 291K, it was observed that the crystal needs about 5 minutes to adjust its water content to changes of relative humidity.<sup>8</sup> Under these conditions, the average distance that a water molecule must diffuse to enter and equilibrate or to leave the crystal is about 0.15 mm. Thus, the corresponding value of a one-dimensional diffusion process along the main direction of diffusion can be estimated to be:

$$D = \frac{\langle x^2 \rangle}{2t} = \frac{(1.5 \cdot 10^6 \text{ \AA})^2}{2 \cdot (3 \cdot 10^{14} \text{ ps})} = 0.00375 \text{ \AA}^2/\text{ps} \quad (10)$$

This value of the diffusion constant is 1/56 of the value in bulk water at room temperature, which is  $0.21 \text{ \AA}^2/\text{ps}$ <sup>21</sup> at 294K and is in fairly good agreement with the value of  $0.007 \text{ \AA}^2/\text{ps}$  obtained for the main diffusion pathway at the higher temperature of about 320K (Figure 6). At that temperature, the experimental diffusion constant of bulk water is about  $0.37 \text{ \AA}^2/\text{ps}$ .<sup>21</sup> The corresponding reduction factor of the calculated diffusion constant then amounts to 1/53, which is even closer to the estimated value of 1/56.

Because in a preliminary evaluation we found no significant differences of the main diffusion pathway at the five different relative humidities considered, the data from the five different MD simulations are lumped together to determine the diffusion pathway. A schematic representation of the main diffusion pathway of water molecules is shown in Color Plate 2 as a red pipeline. This pathway is a global representation of a bundle of many similar pathways, which were calculated with the algorithms described in the Methods section. The gray transparent bodies in Color Plate 2 characterize the locations of the  $\beta$ -CD molecules in the crystal. The main direction of the diffusion path is parallel to the b-axis of the unit cell. The pathway winds through the cavities of the  $\beta$ -CD molecules, as has been proposed based on the crystal structure. The positions of the water molecules in the crystal structure are indicated as blue spheres. During the MD simulation of crystalline  $\beta$ -CD hydrates, all water molecules outside the  $\beta$ -CD ring structure exchange their position with water molecules inside of the ring of the corresponding  $\beta$ -CD molecule. Thus, all water molecules outside of the  $\beta$ -CD ring structure have the possibility to reach the main diffusion pathway easily, and one may assume that the equilibration of crystal water displaced from the main diffusion pathway is fast compared to the time range of minutes needed for equilibration of water molecules in the macroscopic crystalline sample. This is in agreement with mass spectrometric experiments, where it was found that all  $\text{H}_2^{16}\text{O}$  molecules in crystalline  $\beta$ -CD hydrates can be exchanged by  $\text{H}_2^{18}\text{O}$  via solid state diffusion.<sup>9</sup>

## SUMMARY

The transport of water molecules through the crystal lattice of hydrated  $\beta$ -CD was characterized by MD simulation. Trajectories of crystal models consisting of 24  $\beta$ -CD molecules were generated at five different relative humidities with a time period of 4 ns each. According to the time evolution of temperature and RMSD from the crystal structure, the MD simulation data were equilibrated after 1 ns and provided stable and reliable structural data.

Special algorithms were developed to calculate the spatially dependent diffusion constant and the main diffusion direction. Although there is no permanent water channel visible in the crystal structure of  $\beta$ -CD, samples of crystalline  $\beta$ -CD adjust rapidly at room temperature to a change in the ambient relative humidity corresponding to a diffusion constant with a value of about 1/56 of the value in bulk water.<sup>9</sup> The diffusion constant evaluated from the MD simulation data at 320K has a value of  $0.007 \text{ \AA}^2/\text{ps}$ , which is 1/30 of the value in bulk water at room temperature and 1/53 of the value at 320K. The main diffusion pathway is parallel to the crystallographic axis b, and it winds

through the cavities of the  $\beta$ -CD molecules forming the crystal lattice. The water molecules outside of the main diffusion pathway have easy and fast access to this pathway. No significant variation of the diffusion constants and pathways with the relative humidity of crystalline  $\beta$ -CD was found.

## ACKNOWLEDGMENT

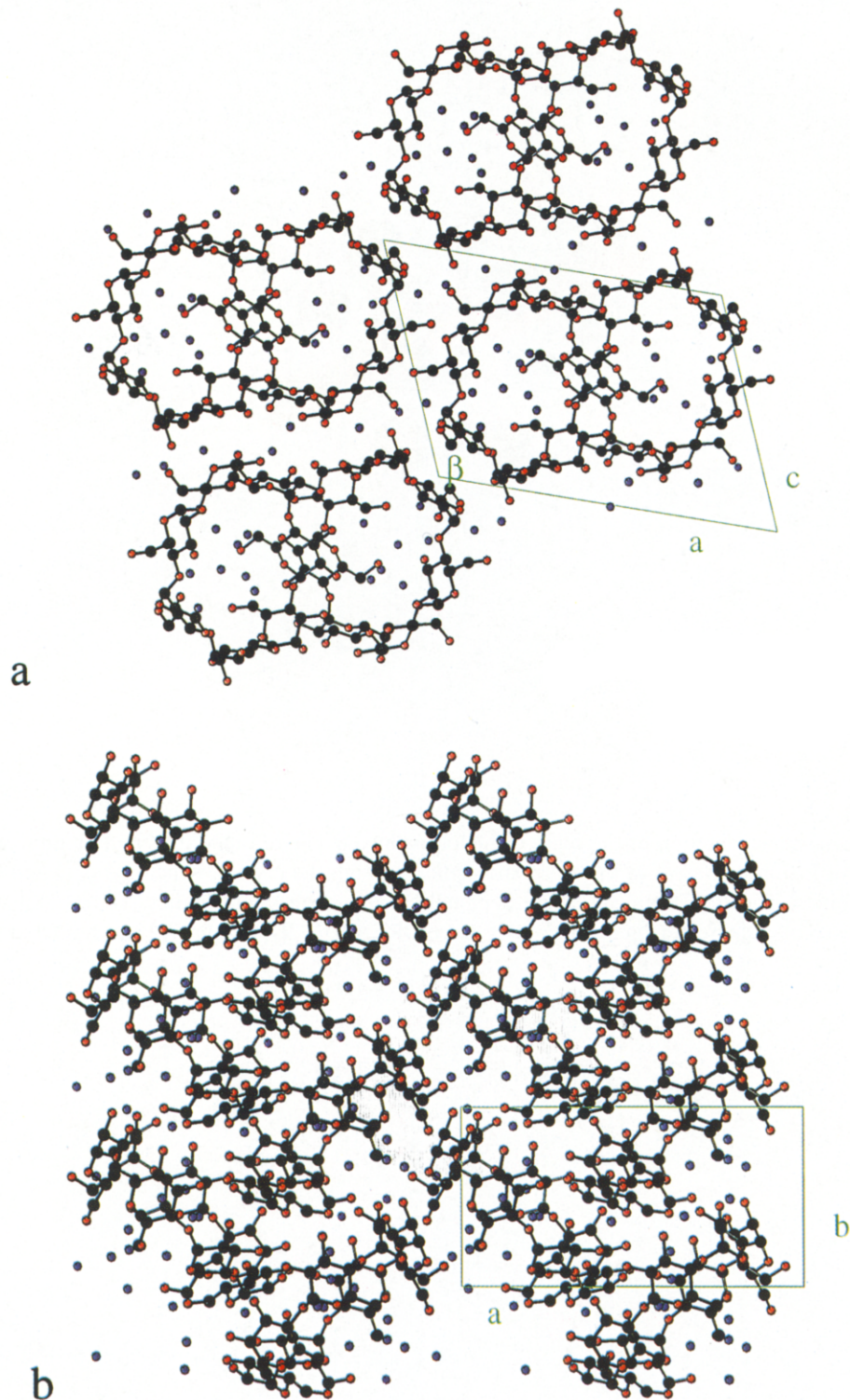
This work was supported by a fellowship to K.B. in the graduate college GRK 80/2 financed by the DFG.

## REFERENCES

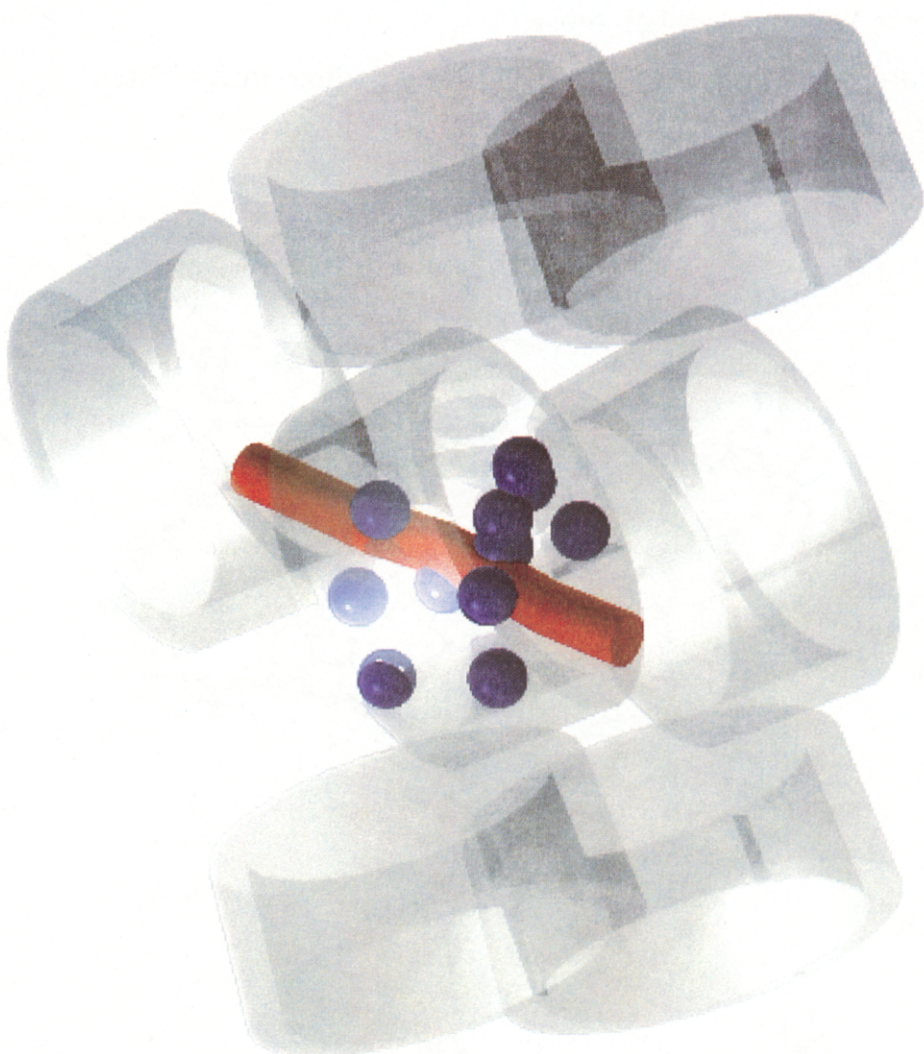
- D'Souza, V.T., and Lipkowitz, K.B., Eds. *Cyclodextrins. Chem. Rev.* 1998, **98**, 1741–2076
- Bender, M.L., and Komiyama M. *Cyclodextrin chemistry*. Springer-Verlag, Berlin, 1978
- Saenger, W. *Cyclodextrins in research and industry*, *Angew. Chem. Int. Ed. Engl.* 1980, **19**, 344–362
- Szejtli, J. *Cyclodextrin technology*. Kluwer, Dordrecht, 1988
- Betzel, C., Saenger, W., Hingerty, B.E., and Brown, G.M. Circular and flip-flop hydrogen bonding in  $\beta$ -cyclodextrin undecahydrate: A neutron diffraction study, *J. Am. Chem. Soc.* 1984, **106**, 7545–7557
- Zabel, V., Saenger, W., and Manson, S.A. Neutron diffraction study of hydrogen bonding in  $\beta$ -cyclodextrin undecahydrate at 120K: From dynamic flip-flop to static homodromic chains, *J. Am. Chem. Soc.* 1986, **108**, 3664–3673
- Steiner, T., Saenger, W., and Lechner, R.E. Dynamics of orientationally disordered hydrogen bonds and of water molecules in a molecular cage. A quasi-elastic neutron scattering study of  $\beta$ -cyclodextrin 11H<sub>2</sub>O. *Mol. Phys.* 1991, **72**, 1211–1232
- Steiner, T., and Koellner, G. Crystalline  $\beta$ -cyclodextrin hydrate at various humidities: Fast, continuous, and reversible dehydration studied by X-ray diffraction. *J. Am. Chem. Soc.* 1994, **12**, 5122–5128
- Steiner, T., da Silva, A.M.M., Teixeira-Dias, J.J.C., Müller, J., and Saenger, W. Rapid water diffusion in a cage-type crystal lattice:  $\beta$ -Cyclodextrin dodecahydrate. *Angew. Chem. Int. Ed. Engl.* 1995, **34**, 1452–1453
- Köhler, J., Saenger, W., and van Gunsteren, W.F. Molecular dynamics simulation of crystalline  $\beta$ -cyclodextrin dodecahydrate at 293 K and 120 K. *Eur. Biophys. J.* 1987, **15**, 211–224
- Brooks, B.R., Bruccoleri, R.E., Olafson, B.D., States, D.J., Swaminathan, S., and Karplus, M. CHARMM: A program for macromolecular energy, minimization, and dynamics calculation, *J. Comput. Chem.* 1983, **4**, 187–217
- MacKerell, A.D., Bashford, D., Bellot, M., Dunbrack, R.L., Evanseck, J.D. Jr., Field, M.J., Fischer, S., Gao, J., Guo, H., Ha, S., Joseph-McCarthy, D., Kuchnir, L., Kuczera, K., Lau, F.T.K., Mattos, C., Michnick, S., Ngo, T., Nguyen, D.T., Prodhom, B., Reiher, W.E., Roux, B., Schlenkrich, M., Smith, J.C., Stote, R., Straub, J., Watanebe, M., Wiorkiewicz-Kuczera, J., Yin, D., and Karplus, M. All-atom empirical potential for molecular modeling and dynamics studies of proteins. *J. Phys. Chem. B* 1998, **102**, 3586–3616

- 13 Berendsen, H.J.C., Grigera, J.R., and Straatsma, T.P. The missing term in effective pair potentials. *J. Phys. Chem.* 1987, **91**, 6269–6271
- 14 SPARTAN, version 4.0, 1995, Wavefunction, Inc., Irvine, CA
- 15 Blumhagen, K., Muegge, I., and Knapp, E.W. Diffusion of two different water models and thermal conductivity in a protein-water system. *Int. J. Quant. Chem.* 1995, **59**, 271–279
- 16 Ryckaert, J.C., Ciccotti, G., and Berendsen, H.J.C. Numerical integration of the cartesian equations of motion of a system with constraints: Molecular dynamics of n-alkanes. *J. Comp. Phys.* 1977, **23**, 327–341
- 17 Knapp, E.W., and Muegge, I. Heterogeneous diffusion of water at protein surfaces: Application to BPTI. *J. Phys. Chem.* 1993, **97**, 11339–11343
- 18 Allen, M.P., and Tildesley, D.J. *Computer simulation of liquids*. Oxford Science Publications, New York, 1996
- 19 Kabsch, W. A solution for the best rotation to relate two sets of vectors. *Acta. Cryst. A* 1976, **32**, 922–923
- 20 Rupley, J.A., and Careri, G., Enzyme hydration and function. In: *The enzyme catalysis process. Energetics, mechanism and dynamics*, Cooper, A., Houben, J.L., and Chien, L.C., Eds., Plenum Press, New York, 1989, pp. 223–234
- 21 Mills, R. Self-diffusion in normal and heavy water in the range 1–45°. *J. Phys. Chem.* 1973, **77**, 685–688

## Diffusion of water molecules in crystalline $\beta$ -cyclodextrin hydrates



Color Plate 1. Top view (a) and side view (b) of the crystalline system of 24  $\beta$ -CD molecules at 100% relative humidity.<sup>8</sup> Carbon atoms are shown in black, oxygen atoms of the water molecules in blue, and all other oxygen atoms in red. Hydrogen atoms are not drawn. The unit cell of the crystal is depicted by green lines.



Color Plate 2. Schematic representation of the main diffusion pathway. The red tube traversing a unit cell is defined by the bundle of individual diffusion pathways of the water molecules through the crystal, which are obtained from the simulation data at all five humidities. The  $\beta$ -CD molecules are depicted by gray transparent bodies. The crystal water molecules are shown as blue spheres. The graphic was generated using CorelDRAW<sup>TM</sup> 3D version 7.0 and rendered with CorelPHOTO-PAINT<sup>TM</sup> version 7.0.